© 2015. Published by The Company of Biologists Ltd | Journal of Cell Science (2015) 128, 3345-3355 doi:10.1242/jcs.174177

RESEARCH ARTICLE

Promotion of periostin expression contributes to the migration of Schwann cells

Eva Sonnenberg-Riethmacher[1,2,*], Michaela Miehe[2,3,*] and Dieter Riethmacher[1,2,‡]

ABSTRACT

Neuregulin ligands and their ErbB receptors are important for the development of Schwann cells, the glial cells of the peripheral nervous system (PNS). ErbB3 deficiency is characterized by a complete loss of Schwann cells along axons of the peripheral nerves, impaired fasciculation and neuronal cell death. We performed comparative gene expression analysis of dorsal root ganglia (DRG) explant cultures from ErbB3-deficient and wild-type mice in order to identify genes that are involved in Schwann cell development and migration. The extracellular matrix (ECM) gene periostin was found to exhibit the most prominent down regulation in ErbB3-deficient DRG. Expression analysis revealed that the periostin-expressing cell population in the PNS corresponds to Schwann cell precursors and Schwann cells, and is particularly high in migratory Schwann cells. Furthermore, stimulation of Schwann cells with neuregulin-1 (NRG1) or transforming growth factor β (TGFβ-1) resulted in an upregulation of periostin expression. Interestingly, DRG explant cultures of periostin-deficient mice revealed a significant reduction of the number of migrating Schwann cells. These data demonstrate that the expression of periostin is stimulated by ErbB ligand NRG1 and influences the migration of Schwann cell precursors.

KEY WORDS: Periostin, Schwann cells, Migration, Neuregulin, Dorsal root ganglia, ECM

INTRODUCTION

Schwann cell precursors and PNS sensory neurons originate from the neural crest. The neural crest cells that are fated to participate in the formation of dorsal root ganglia (DRG) migrate through the rostral half of each somite and condense in repetitive units on both sides of the spinal cord. These nascent sensory ganglia comprise neural and glial progenitors with heterogeneous developmental potentialities. Upon differentiation of sensory neurons and axonal outgrowth, Schwann cell precursors migrate from the DRG along these projections. Later in development they differentiate into myelinating or non-myelinating Schwann cells that envelope sensory- and motor-neuron axons. The development of peripheral nerve tissue results from a series of coordinated interactions between neurons and Schwann cells (Jessen and Mirsky, 2005). Targeted mutagenesis of different components of the ErbB-signalling complex has demonstrated its importance for Schwann cell development (Britsch et al., 1998; Garratt et al., 2000; Michailov et al., 2004; Riethmacher et al., 1997; Taveggia et al., 2005). Those experiments revealed that, later in development, mutant embryos exhibit a total loss of Schwann cells along their peripheral axons, whereas pre-migratory Schwann cells are present near to the dorsal root ganglia but fail to migrate along the axons. The impaired glial cell migration in these mutants indicates a direct function in migration. This interpretation is supported by the finding that mutations in the neuregulin–ErbB signalling system lead to changes in neural crest migration in mice (Britsch et al., 1998) and in directed Schwann cell migration in zebrafish (Lyons et al., 2005). However, an earlier function in fate specification and/or proliferation that could in turn be a prerequisite for migration cannot be completely ruled out.

To identify components that are potentially involved in the migration process of Schwann cells, we took advantage of the impairment of Schwann cell migration in ErbB3-deficient embryos. We conducted gene expression profiling of cultured embryonic DRG [12.5 days post coitum (dpc)], isolated from wild-type and ErbB3-deficient embryos. Aiming to identify genes expressed by migrating Schwann cells, we have been focusing on genes that are upregulated in wild-type compared with mutant cultures, because the wild-type cultures are enriched for migrating Schwann cell precursors as opposed to those that are immobile. Periostin was one such gene that showed a higher expression in wild-type compared with ErbB3-deficient cultures.

Periostin was originally isolated from osteoblasts and found to be preferentially expressed in the periosteum, hence the name (Horiuchi et al., 1999; Takeshita et al., 1993). Periostin contains an N-terminal secretory signal peptide, followed by a cysteine-rich domain, four internal homologous repeats and a C-terminal hydrophilic domain. The four internal repeats region, the fasciclin domains (Fas), exhibit homology to the axon guidance protein Fasciclin I that is involved in the development of nervous system in invertebrates (Zinn et al., 1988). Interestingly, in invertebrates, it is expressed in neurons and attached to the membrane through a glycosylphosphatidylinositol (GPI) anchor (Elkins et al., 1990), whereas in vertebrates, it is a secreted protein with a much broader expression pattern – including heart, periodontal ligament, fibroblasts and Schwann cells. In primary osteoblasts, periostin expression can be increased through stimulation with TGFβ-1 (Horiuchi et al., 1999). Several studies aiming to locate the protein product have revealed its presence in the ECM surrounding the expressing cells. In the ECM, periostin seems to be able to interact with several other ECM molecules, including collagen and tenascin-C (Kii et al., 2006, 2010). Furthermore, it has been demonstrated that periostin promotes adhesion and potentiates cancer cell motility by binding to integrins $\alpha_v\beta_3$ and $\alpha_v\beta_5$ (Gillan et al., 2002), and that forced expression of periostin induces invasive activity through epithelial–mesenchymal transition (EMT) in HEK-293 cells (Yan and Shao, 2006). Several studies correlate periostin expression with tumour angiogenesis and metastasis in human

[1]Human Development and Health, University of Southampton, School of Medicine, Tremona Road, Southampton SO16 6YD, UK. [2]Center for Molecular Neurobiology, University of Hamburg, Falkenried 94, Hamburg 20251, Germany. [3]Institut for Immunological Engineering, University of Aarhus, Gustav Wieds Vej 10, Aarhus C 8000, Denmark.
*These authors contributed equally to this work

‡Author for correspondence (d.riethmacher@soton.ac.uk)

Received 8 May 2015; Accepted 25 June 2015

Journal of Cell Science

Journal of Cell Science (2015) 128, 3345-3355 doi:10.1242/jcs.174177

cancer (Bao et al., 2004; Li et al., 2007; Malanchi et al., 2011; Puglisi et al., 2008; Sasaki et al., 2001a,b, 2003). Additionally, high pre-operative serum levels of periostin correlate with a poor prognosis in individuals with hepatocellular carcinoma after hepatectomy (Lv et al., 2013). Based on these observations, it has been suggested that periostin belongs to the group of matricellular proteins that are characterised as being modulators of cell-matrix interactions and cellular function (Kii et al., 2010; Norris et al., 2008). Interestingly, the existence of a non-secreted intracellular pool of periostin that is able to suppress the invasiveness of cancer cells, possibly by interacting with intracellular signalling molecules such as TAB1 and Tak1, has also been described (Isono et al., 2009; Yoshioka et al., 2002). In our current study, we show that periostin expression is downregulated in ErbB3-deficient DRG. In cultured rat Schwann cells, expression of periostin can be induced by neuregulin-1 (NRG1) and TGFβ-1. Additionally, we demonstrate that periostin deficiency leads to reduced migration of embryonic Schwann cell precursors and that recombinant periostin is able to promote cellular motility.

RESULTS

Genes expressed in migrating Schwann cell precursors

In order to identify genes that are potentially involved in Schwann cell precursor migration, we performed DNA microarray expression analysis with DRG explant cultures of ErbB3-deficient embryos. In mutant cultures, the migration of Schwann cell precursors along the axons did not occur, yet axonal outgrowth and neuronal survival in these cultures was not impaired (Fig. 1A). At 12.5 dpc, the DRG of ErbB3-deficient and wild-type embryos were isolated. Following 36 h of *in vitro* culture, the explant cultures were harvested, RNA was isolated and then used to hybridize Affymetrix MicroArray (probe sets MG-U74Av2, MG-U74Bv2 and MG-U74Cv2). After evaluation of the obtained data sets, 176 genes were found to exhibit a significantly higher expression in samples that had been derived from wild-type DRG cultures, in contrast, only nine genes showed increased expression in samples from ErbB3-deficient DRG. To further analyse the data, we grouped the differentially expressed genes into functional categories. The three major groups were transcription-related proteins, ECM proteins and nuclear proteins (Fig. 1B). However, when we focused our analysis on genes that exhibited the most significant increases in expression in wild-type DRG (top 20 of the list), 36% (7 out of 20) could be assigned to the group of the ECM proteins (Fig. 1C).

The most prominent differential expression was detected for the ECM molecule periostin. To verify and further support this finding, we next compared expression levels by using other approaches. A virtual northern blot analysis employing the total RNA of DRG explant cultures derived from wild-type and ErbB3-deficient cultures confirmed the lower expression levels of periostin in ErbB3-deficient cultures (Fig. 1D). Moreover, quantitative real-time PCR (qRT-PCR) analysis revealed a 10.5-fold higher expression of periostin in samples derived from wild type compared with those from mutant cultures (data not shown). As the most prominent difference between wild-type and ErbB3-deficient DRG cultures is the population of migrating Schwann cell precursors, these results point towards expression in these cells and also suggest a potential role of periostin for the migration process of these cells.

Periostin expression in Schwann cells

We therefore analysed the expression pattern of periostin during embryonic development by using *in situ* hybridisation of wild-type embryos at different stages. Prominent periostin expression is detectable in a variety of tissues and organs including bone, cartilage, heart and tongue as early as 10.5 dpc. At this stage of development, neural crest cells have already migrated out of the neural tube, and DRG formation has been initiated. Periostin expression was readily detectable in DRG at this early stage (Fig. 2A), and expression within DRG persists throughout embryonic development (Fig. 2B,C). At 12.5 dpc, strong expression of periostin could additionally be detected along axonal projections (Fig. 2D). To further characterise the expression pattern, we made use of a mouse mutant in which the β-galactosidase open reading frame had been fused in frame to the ATG start codon of the periostin gene, thereby replacing most of exon 1 and exon 2, resulting in a frameshift (the generation of these mice will be described elsewhere). Heterozygous animals were phenotypically normal but expressed the β-galactosidase gene within the cells that expressed periostin. Co-immunofluorescence

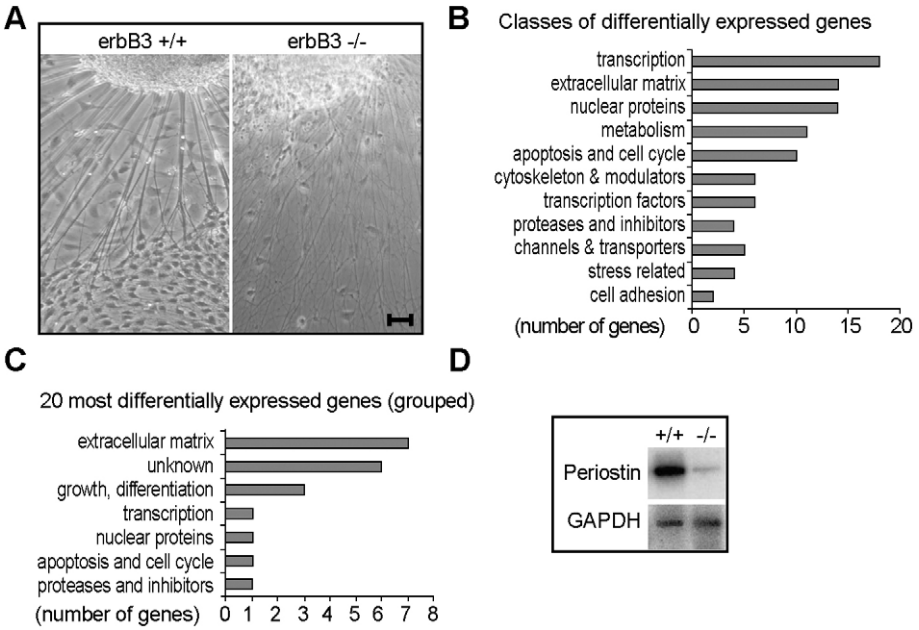

Fig. 1. Microarray analysis of DRG explant cultures of wild-type and ErbB3-deficient mice. (A) DRG explant cultures of wild-type (+/+) and ErbB3-deficient mice (–/–) were isolated from embryos at 12 dpc, cultured for 72 h and imaged under a microscope using phase contrast. Note the absence of migrating Schwann cells in the DRG culture from ErbB3–/– animals. Scale bar: 50 µm. (B) All genes with a higher level of expression in wild-type DRG were grouped into functional categories. (C) Twenty genes with the highest differential expression were grouped into classes. Note the high percentage of ECM molecules (7 out of 20, 35%). (D) Virtual northern blot of mRNA isolated from DRG explant cultures of wild-type (+/+) and ErbB3-deficient mice (–/–). The periostin-specific transcript was detected through hybridisation with a radioactively labelled periostin-specific probe. GAPDH was detected accordingly and was employed as a loading control.

Journal of Cell Science (2015) 128, 3345-3355 doi:10.1242/jcs.174177

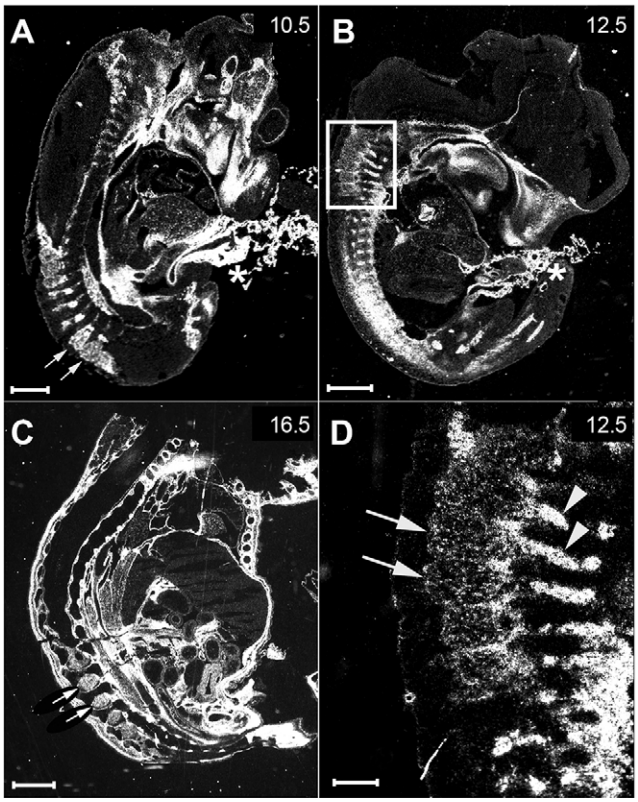

Fig. 2. Expression analysis of periostin in DRG. (A–D) Periostin expression during development was followed by using *in situ* hybridisation with a ^{35}S-labelled periostin-specific probe on sagittal sections of wild-type embryos at different stages. Expression in several connective tissues, the periosteum and the valves of the heart has been previously described. Also note the strong expression in the umbilical cord, highlighted with an asterisk (A,B). (A) Expression at 10.5 dpc. Note the expression in the DRG, indicated by arrows. (C) Expression at 16.5 dpc shows that the robust expression within the DRG persists (arrows). (B,D) Expression at 12.5 dpc. D is a higher magnification of the boxed area in B. Note the higher expression along axonal projections (arrowheads) compared with the expression level within the DRG (arrows). Scale bars: 250 µm (A); 500 µm (B,C); 125 µm (D).

analysis of heterozygous embryos at 12.5 dpc with antibodies specific for β-galactosidase and Sox10, a marker for glial cells in the PNS, confirmed the expression of periostin in the glial cell population (Fig. 3A–C). To examine the expression pattern of periostin in DRG explant cultures, we performed a co-immunofluorescence analysis that employed antibodies against Sox10 and periostin. Sox10-positive cells were found to exhibit robust periostin expression (Fig. 3D–F). Interestingly, even though the majority of the protein is secreted and can be detected in and purified from the supernatant, periostin was also detected within the cells.

Different isoforms of periostin varying within the 3′-translated region have been described (Horiuchi et al., 1999; Litvin et al., 2004). Interestingly, exon 17 has not been included in the official periostin cDNA or protein sequences; however, it is present in the genome sequence releases and thus should be included. Exon 17 has been described by Litvin et al. as only being present in the isoform periostin-like factor (PLF) (Litvin et al., 2004), whereas Kyutoku et al. correctly state it to be part of the periostin coding region (Kyutoku et al., 2011). To assess the presence of different periostin isoforms in glial cells of the PNS, we generated cDNA from DRG. Amplification by using gene-specific primers and subsequent

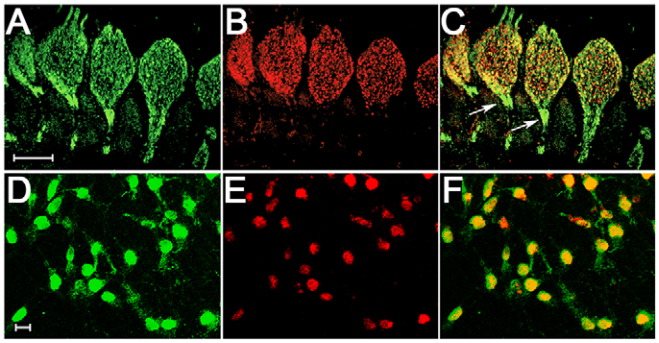

Fig. 3. Co-expression of periostin and Sox10 in DRG and DRG explant cultures. (A–C) Periostin expression in DRG was analysed by using immunohistochemistry analysis of sagittal sections of heterozygous periostin-mutant embryos at 12.5 dpc. (A) To identify cells that expressed periostin, we made use of the β-galactosidase (green) expression, which reflects the periostin expression in heterozygous periostin mutants. Note that the β-galactosidase remained within the expressing cells in contrast to periostin, which was secreted. (B) Glial cells were identified through expression of the glial marker Sox10 (red). (C) An overlay of the images in A and B is shown. Note the strong expression of periostin (β-galactosidase) in the area of the nerve root (arrows). (D–F) Periostin expression in DRG explant cultures was assessed by co-immunostaining with antibodies against periostin (green, D) and Sox10 (red, E). An area several millimetres away from the ganglia, where mostly migrating Sox10-positive Schwann cells are located, is shown. (F) An overlay of the images in D and E is shown. Note the substantial overlap of Sox10 and periostin expression in migrating Schwann cells. Scales bars: 100 µm (A–C); 10 µm (D–F).

sequence analysis revealed the expression of five different isoforms in embryonic glial cells, one of which (isoform IV) was previously unidentified (Fig. 4). We were able to detect a full-length transcript (containing all 23 exons) and several variants where either exon 21 (isoform II) or 17 (isoform III) were absent, or a combination of exons 17 and 20 (isoform IV) or exon 17, 20 and 21 (isoform V) were absent (Fig. 4).

Relocalisation of periostin through neuregulin-1 and stimulation of periostin transcription in Schwann cells

As we identified periostin in our screen as being upregulated in wild-type DRGs compared with ErbB3-deficient DRGs, we next investigated whether the neuregulin–ErbB signalling system has any direct influence on periostin expression levels. For these experiments, we used the S16 Schwann cell line, which closely corresponds to Schwann cells at an early stage of myelination (Toda et al., 1994). These cells express the ErbB receptors and are responsive to NRG1 (data not shown). S16 cells were grown either on laminin or on poly-DL-ornithine (PDO), and left unstimulated or were stimulated with NRG1. In cells grown on PDO, non-secreted periostin localized in the centre of the cytoplasm, surrounding the nucleus (Fig. 5A), whereas in cells grown on laminin, periostin was observed mainly at the protrusions of the cells (Fig. 5C). Interestingly, upon stimulation with NRG1, expression levels appeared to be upregulated and the protein localized at cellular protrusions, whether cells were grown on PDO or laminin (Fig. 5B,D). Thus, the stimulation with NRG1 of S16 Schwann cells that had been grown on PDO resulted in a relocalisation of periostin, reminiscent of the localisation of the protein that was observed when cells were grown on a migration-promoting surface such as laminin.

To assess the impact of NRG1 stimulation on periostin expression levels, we performed a qRT-PCR analysis. S16 cells were cultured until they were semi-confluent and then stimulated with NRG1, TGFβ-1 or a mixture of both factors. TGFβ-1 is a known stimulator

Journal of Cell Science (2015) 128, 3345-3355 doi:10.1242/jcs.174177

A

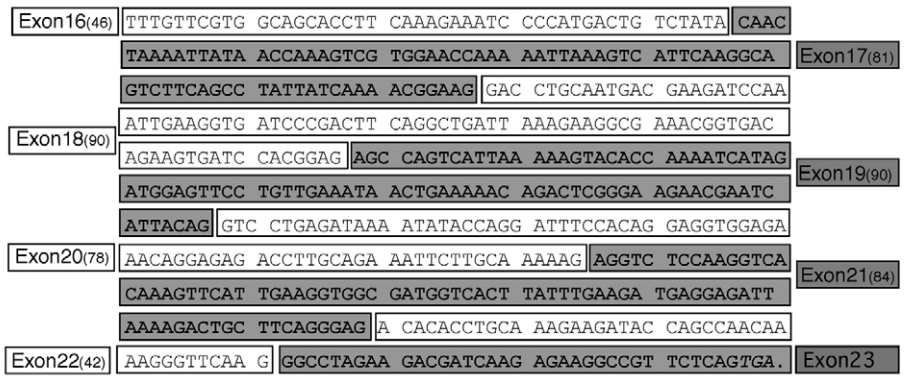

B

Isoform	Exon	length of cDNA in bp	amino acid	kDa
I	16 17 18 19 20 21 22 23	2514	838	93,14
II	16 17 18 19 20 --- 22 23	2430	810	89,98
III	16 --- 18 19 20 21 22 23	2433	811	90,26
IV	16 --- 18 19 --- 21 22 23	2355	785	87,10
V	16 --- 18 19 --- --- 22 23	2271	757	84,28

Fig. 4. Periostin isoforms in wild-type DRG explant cultures. (A) Nucleotide sequence of the C-terminal domain of murine periostin. Exons 16 to 23 (up to the stop codon) are shown. The exons are boxed and alternate between white (even) and grey (odd). The exon lengths (number of nucleotides) are indicated in brackets. Note that excision of any exon from exon 17 to exon 22 does not induce a frameshift. (B) Isoforms identified in wild-type DRG explant cultures are shown, depicting exon composition, length and calculated molecular mass. For this analysis, mRNA of DRG explant cultures that had been cultured for 3 days was isolated, then cDNA was generated and amplified with specific primer sets F15 (forward primer exon 15) and R23 (reverse primer exon 23), subcloned and sequenced. In all variants, exons 16, 18, 19, 22 and 23 were present. Note that variant IV has not been described before.

of periostin expression in a variety of cell types (Horiuchi et al., 1999; Tai et al., 2005). Stimulation with NRG1 resulted in an almost fivefold increase of periostin expression, whereas stimulation with TGFβ-1 resulted in a sixfold increase compared with that of unstimulated cells (Fig. 5E). Interestingly, we observed an 11-fold increase of periostin transcription levels upon combined stimulation with both NRG1 and TGFβ-1 (Fig. 5E), suggesting that the ErbB3 ligand NRG1 and TGFβ-1 cooperate to upregulate periostin expression in S16 Schwann cells.

Periostin interacts with laminin and a variety of ECM molecules

Periostin is known to interact with collagen I (Norris et al., 2007), as well as other ECM molecules such as fibronectin, tenascin-C and collagen IV (Kii et al., 2010; Takayama et al., 2006). The relocalisation of periostin in S16 Schwann cells that had been cultured on laminin prompted us to investigate whether periostin and laminin can interact directly. In order to test such a potential interaction, a His_{10}- and c-Myc double-tagged recombinant periostin construct (isoform I, full length) was expressed in HEK-293 cells and purified to homogeneity from cellular supernatants by using Ni^{2+}-affinity chromatography, as assessed by using SDS-PAGE and western blotting (Fig. 6A). Solid-phase binding assays demonstrated a robust interaction of recombinant periostin with laminin and a less pronounced interaction with collagen I and fibronectin (Fig. 6B). This interaction was dependent on the presence of Ca^{2+} because without added Ca^{2+}, no specific interaction could be detected (data not shown). We were unable to observe any specific interaction with collagen IV (Fig. 6B). To further corroborate this interaction between periostin and laminin, we performed co-immunoprecipitation experiments with periostin-expressing cells and exogenously added laminin. In these experiments we were able to co-precipitate periostin by using laminin-specific antibodies (Fig. 6C). Having demonstrated the potential of the two proteins to physically interact, we determined their location in developing nerves. We were able to co-localise both proteins in developing nerves by employing sections of DRG and spinal nerves from 12.5-dpc embryos (Fig. 7A). Co-localization and the ability to physically interact indicate that there is a functional interplay between the two molecules *in vivo*.

Periostin stimulates migration of Schwann cell precursors and HEK-293 cells

Because we discovered periostin in an expression analysis that aimed to identify genes which are potentially involved in Schwann cell migration, we next examined the effect of periostin expression on Schwann cell migration. To this end, we used embryonic DRG cultures from periostin-deficient and wild-type mice and compared Schwann cell migration. Several groups, including ours, have independently generated periostin-deficient animals (Kii et al., 2006; Oka et al., 2007; Rios et al., 2005) (A. Brodarac, Impaired tooth development in periostin deficient mice, PhD thesis, University of Hamburg, 2006). These mice do not show any overt phenotype during embryonic development, and the gross development of the PNS appears normal in the absence of periostin expression. Interestingly, when we analysed DRG cultures, we observed severely reduced migration of Sox10-positive Schwann cells in periostin-deficient cultures compared with that in wild-type cultures, whereas the axon outgrowth was not impaired (Fig. 7B). To characterise this in more detail, we monitored migration in several independent cultures from wild type, and heterozygous and homozygous periostin mutants. Schwann cell migration in cultures from heterozygous mutants was normal, whereas

Journal of Cell Science (2015) 128, 3345-3355 doi:10.1242/jcs.174177

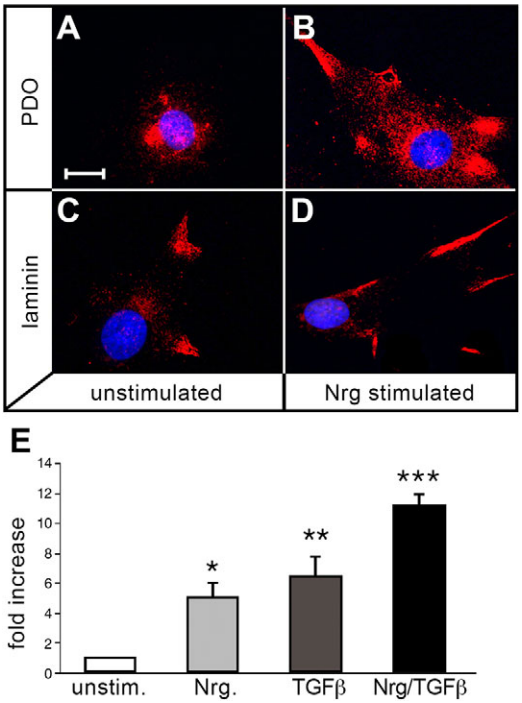

Fig. 5. Expression analysis of periostin in S16 Schwann cells. (A–D) Periostin expression in S16 cells was analysed by using immunocytochemistry with a periostin-specific antibody (red). Nuclei were visualized by Hoechst 33342 staining. S16 cells were plated on poly-DL-ornithine (PDO)- (A,B) or laminin-coated (C,D) dishes, cultured with serum-free medium and then treated with 10 ng/ml NRG1 (Nrg) for 4 h (B,D) or the treatment with NRG1 was omitted (unstimulated) (A,C). Note the relocalisation of periostin upon NRG1 stimulation on PDO (B). Expression of periostin appears to be upregulated upon stimulation with NRG1 on both substrates. Scale bar: 10 µm (A–D). (E) To analyse the upregulation in more detail, S16 cells were plated on laminin-coated dishes, cultured with serum-free medium and stimulated for 24 h with 10 ng/ml NRG1 (Nrg) or 1 ng/ml TGFβ-1 (TGFβ), a known stimulator of periostin expression in a variety of cell types. Periostin transcript levels were analysed by using qRT-PCR for three independent experiments. A strong and significant increase in periostin expression could be observed after stimulation with NRG1, TGFβ-1 or stimulation with both (Nrg/TGFβ) compared with that of unstimulated cells (unstim.). Significance is indicated as **P*<0.05, ***P*<0.01, ****P*<0.001.

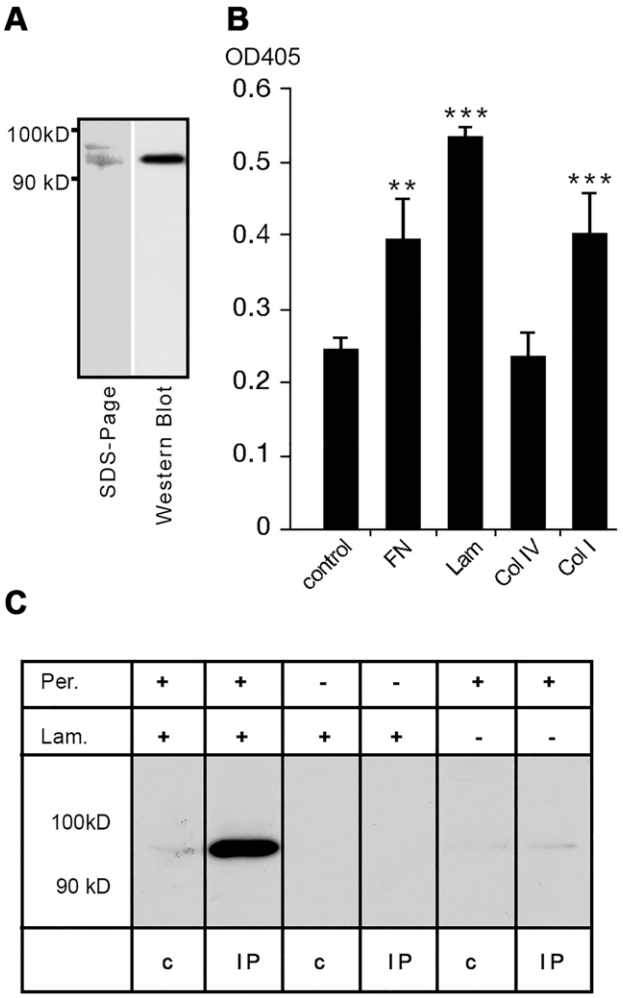

Fig. 6. Interaction of periostin with ECM molecules. (A) Periostin comprising a C-terminal His-tag and an additional c-Myc epitope was expressed in HEK-293 cells and purified by using Ni^{2+} affinity chromatography. Coomassie-stained SDS-PAGE and immunoblotting using a Myc-specific antibody revealed a protein with a molecular mass in the expected range of slightly above 90 kDa. (B) Interaction of periostin with ECM molecules was analysed by using a solid-phase assay. 100 µg/ml of the ECM molecules were coated onto 96-well plates and incubated with 50 µg/ml recombinant periostin in the presence of Ca^{2+} in the binding buffer. Interaction of periostin was detected using an anti-c-Myc HRP conjugate and visualized using ABTS as a substrate. Note that the interaction was Ca^{2+}-dependent as binding in the absence of Ca^{2+} was below the control level and did not vary between the different ECM molecules. Significance is indicated as ***P*<0.01, ****P*<0.001. FN, fibronectin; Lam, laminin; Col, collagen (isoforms IV and I, respectively). (C) Co-immunoprecipitation of laminin (Lam.) and periostin (Per.) was performed in mock (–) or periostin (+) transfected HEK-293 cells. Laminin (+) was added to the supernatant and complexes were precipitated using a laminin-specific antibody. The interaction was assessed by immunoblotting and detection of precipitated periostin with a Myc-specific antibody. The control lanes (c) represent the input before immunoprecipitation, whereas the 'IP' lanes show the results after immunoprecipitation.

in cultures from periostin-deficient embryos, we observed a 50% reduction in migration (Fig. 8A). Attempts to rescue mutant cultures by either prior coating of the dishes with periostin or by adding it to the medium were not successful (data not shown). We next analysed whether periostin deficiency has any impact on Schwann cell proliferation or apoptosis in these cultures as this would also affect the outcome of our migration analysis. However, proliferation and apoptosis rates in wild-type and periostin-deficient DRG cultures showed no significant differences (Fig. 8B). The finding that neither proliferation nor apoptosis were affected in these cultures clearly suggests that periostin has a direct impact on the migratory capacity of Schwann cell precursors.

Because periostin has been implicated in migration processes in a variety of cell types and different contexts (i.e. cancer, cutaneous wound healing), we wanted to support our observations of DRG cultures by employing another experimental setup. Therefore, periostin- or mock-transfected HEK-293 cells were analysed in a Boyden chamber assay using conditioned medium from these cells or control medium that did not contain any periostin (Fig. 8C). In this experimental setup, conditioned medium containing periostin strongly stimulated the migration of HEK-293 cells. Interestingly, migration was highest when cells were exposed to periostin but did not express it endogenously (Fig. 8D), and the observed migration in this experimental setup was regarded as 100%. Periostin-expressing HEK-293 cells exhibited a slightly lower migration rate (80%). When no periostin was present in the medium, mock-transfected (EGFP) control cells were stationary, whereas periostin-expressing cells were still able to migrate (40%) (Fig. 8D). To assess whether this higher migration rate was accompanied by higher rates of proliferation of

Journal of Cell Science (2015) 128, 3345-3355 doi:10.1242/jcs.174177

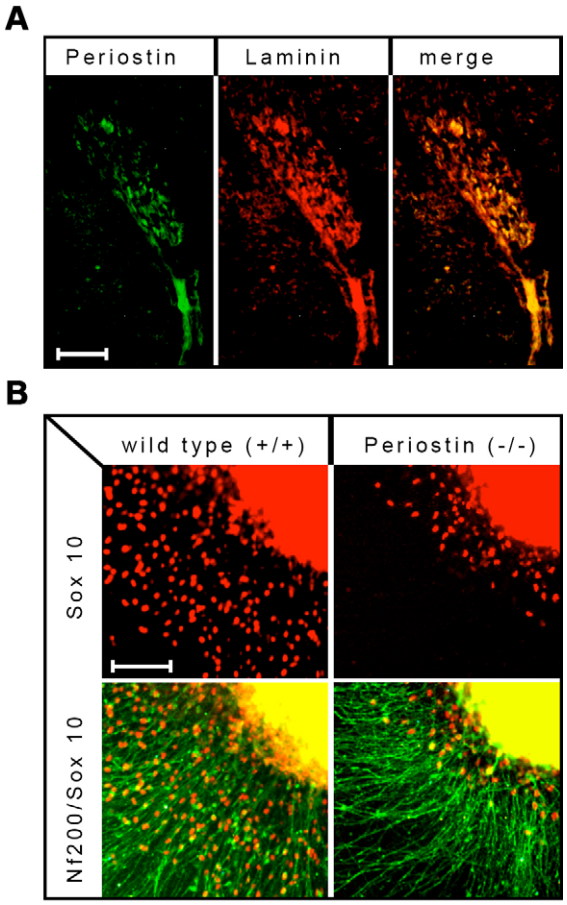

Fig. 7. Colocalisation and influence on migration. (A) Immunostaining of cryosections from a 12.5-dpc embryo showing the area of the thoracic DRG with periostin- (green) and laminin-specific (red) antibodies. Note the substantial overlap of the expression domains, both within the DRG and along the axonal projection. (B) Immunostaining of DRG explant cultures derived from wild-type and periostin-deficient embryos (12.5 dpc) using the Neurofilament200 (Nf200, green) antibody and an antibody specific for Sox10 (red). Axonal projections (lengths and numbers) are comparable between genotypes, whereas the number of migrating Schwann cell precursors (Sox10 positive) is clearly reduced in periostin-deficient cultures. Nf200/Sox10, co-staining of neurofilaments and Sox10. Scale bars: 100 µm (A,B).

these cells, which might influence the migration behaviour, a BrdU labelling experiment was performed. Again, we were unable to detect any changes in the proliferation rates (data not shown). These findings and the results obtained using DRG cultures clearly indicate that periostin can increase the migratory capacity of cells.

DISCUSSION

Considerable progress has been made in the identification of molecules involved in neural crest cell development and in understanding their impact on processes – including proliferation, differentiation and de-differentiation (Crane and Trainor, 2006; Dupin et al., 2007). However, there is only scarce knowledge of the molecules involved in Schwann cell migration. One important player in neural crest and Schwann cell development is the neuregulin–ErbB signalling system (Newbern and Birchmeier, 2010). DRG explant cultures of ErbB3-deficient embryos reflect the migration impairment of the Schwann cell precursor (Riethmacher et al., 1997) and therefore represent an ideal model for expression analyses of the genes that are involved in migration when compared with those of wild-type cultures. Our microarray analyses revealed a prominent differential expression of ECM molecules, which is independently supported by microarray data that has been collected using isolated neural crest stem cells and Schwann cell precursors (Buchstaller et al., 2004). The highly differential expression of ECM molecules coincides with axonal growth and the on-going process of Schwann cell precursor migration along the axons, suggesting a potential involvement of such ECM components in these processes. Furthermore, ECM molecules and their receptors have been implicated in Schwann cell development and function (Chernousov et al., 2008), as well as migration (Chernousov et al., 2001; Milner et al., 1997). The ECM protein periostin, which exhibited the most significant differential expression in our microarray analysis, is expressed in a variety of tissues during development, including DRG and Schwann cell precursors, as shown by us and others (Kruzynska-Frejtag et al., 2001; Lindsley et al., 2005).

So far, several isoforms of periostin with varying domain compositions in the C-terminus, generated through alternative splicing, have been reported (Horiuchi et al., 1999; Litvin et al., 2004; Ozdemir et al., 2014). Using RNA that was isolated from DRG cultures, we could identify five different isoforms, including an isoform that has not been described previously. The exact function and physiological relevance of the different isoforms remain elusive. However, because periostin has been implicated in a variety of different, partially even conflicting, functions (Bao et al., 2004; Kim et al., 2005; Shao et al., 2004), alternative splicing might offer an explanation for these findings. Similarly, the different isoforms present in the precursor and migrating Schwann cells might have varying impacts on cellular behaviour – e.g. motility. Further experiments are required to investigate how different compositions of the C-terminus influence the ability to interact with other ECM molecules or receptors. In this context, it will also be interesting to determine the expression levels of the different splice variants.

In order to identify the biological functions of periostin, several labs have independently generated periostin-deficient mice. Surprisingly, despite the robust expression during embryonic development, mutants show apparently normal development and are viable, indicating that there is a backup mechanism for periostin function in its absence. The most apparent phenotype is impairment of the eruption of incisors, which first presents itself shortly after weaning (A. Brodarac, Impaired tooth development in periostin deficient mice, PhD thesis, University of Hamburg, 2006) and causes secondary defects such as malnutrition and dwarfism (Kii et al., 2006; Rios et al., 2005). More recent studies involving different challenging strategies have revealed subtle defects in skin, tendons, heart valves, and changes in regeneration dynamics following myocardial infarction (Norris et al., 2008, 2007; Oka et al., 2007; Shimazaki and Kudo, 2008; Snider et al., 2008). Interestingly, subtle phenotypes during normal development and impairment of tissue remodelling and repair are hallmarks of mice carrying targeted mutations in other matricellular proteins (Bornstein and Sage, 2002).

Although Schwann cell development is normal in periostin-deficient animals, in this paper we were able to show that cultured DRG of periostin-deficient animals could not sustain Schwann cell migration at levels comparable to those of wild-type DRG. During development, there is most likely to be an alternative mechanism operating in the absence of periostin that is not present in our DRG culture. This experimental setup shows that periostin can be involved in cell migration. Our Boyden chamber assay further showed that the concentration and localisation of periostin is also important for its migratory function. We therefore conclude that periostin can influence the migratory behaviour of Schwann cells and also other cells, but in the absence of periostin, other proteins – i.e. murine TGFBI – can

Journal of Cell Science (2015) 128, 3345-3355 doi:10.1242/jcs.174177

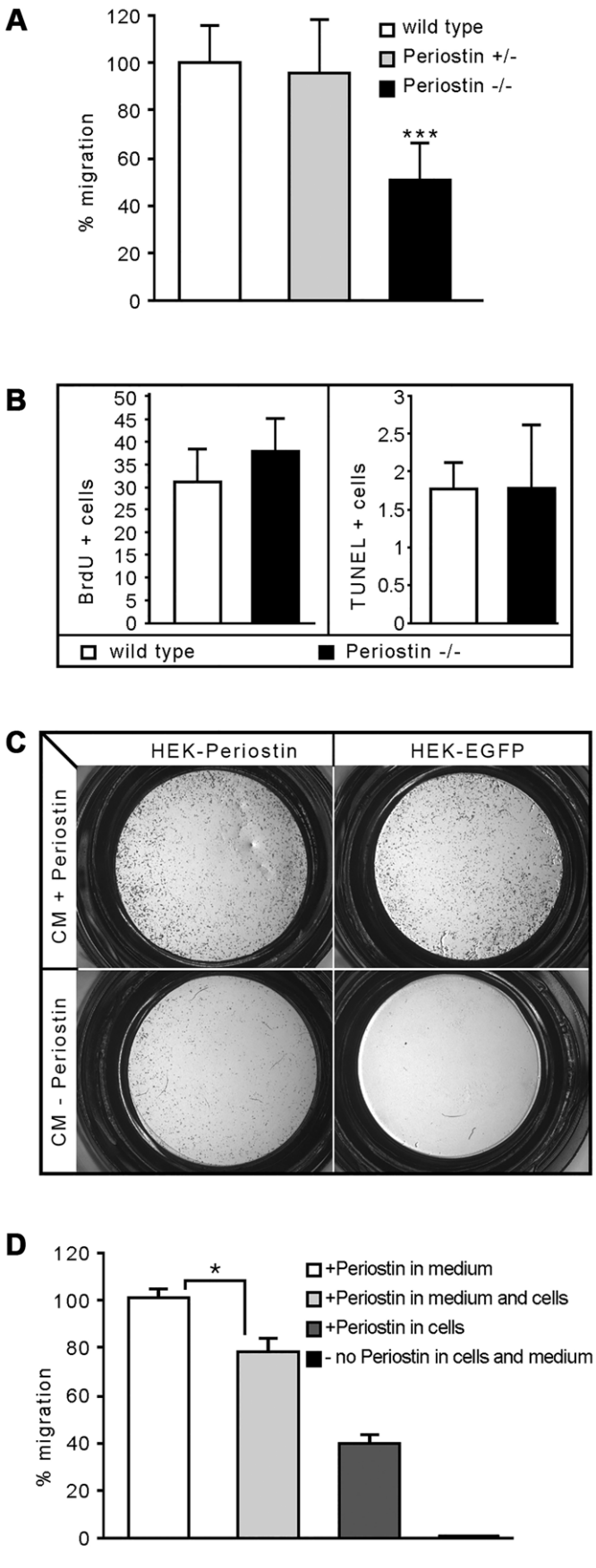

Fig. 8. Influence of periostin on migration. (A) DRG explant cultures from periostin deficient (–/–), heterozygous (+/–) or wild-type (+/+) embryos (12.5 dpc) were cultured for 72 h and stained with an antibody against Sox10 (red) to visualise the Schwann cells (see Fig. 7B). The Sox10-positive migrating cells per DRG were counted in all DRG that had adhered to the coverslip and divided by the number of DRG. The mean number of wild-type cultures was taken as 100% migration and compared with the mean numbers of heterozygous and periostin-deficient cultures. Wild-type and heterozygous cultures showed very similar values, whereas a significant difference (***P<0.001) became apparent in periostin-deficient cultures. (B) Proliferation and apoptosis. Proliferation was followed by treatment of the DRG explant cultures with BrdU for 1 h. Apoptosis was monitored by applying the TUNEL method. Schwann cells were visualized by using a Sox10-specific antibody. The cells positive for both BrdU and Sox10, or TUNEL and Sox10 were counted and related to the total number of Sox10-postitive cells. No significant differences could be detected. (C) Boyden chamber assay. Conditioned medium from HEK-293 cells that either stably expressed periostin (CM+Periostin) or did not express periostin (CM–Periostin) was added to the lower well of a chemotactic chamber. Either periostin (Hek-Periostin) or mock transfected (Hek-EGFP) HEK-293 cells were plated at equivalent densities on the membrane of the upper chamber. After 48 h, the membrane was stained and the cells counted. (D) Several independent assays were performed and statistically analysed. All observed differences were highly significant (***P<0.001, not indicated in graph for clarity). The highest migration activity was observed in experiments when mock-transfected cells were assayed in the presence of periostin in the conditioned medium (white box). These values were taken as 100% and compared with the other values. Interestingly, cells expressing periostin that had been assayed in the presence of periostin in the conditioned medium (light grey) just reach 80% (*P<0.05), suggesting that very high levels of periostin might impede migration. Note that cells expressing periostin are able to migrate in this assay, even when no periostin was added in the conditioned medium (dark grey), whereas no migration was detected when non-expressing cells were assayed in the absence of periostin in the medium (black).

compensate for its function during embryonic development. Interestingly, our preliminary data indicate that the absence of periostin leads to delayed and reduced regeneration after peripheral nerve injury (E.S.-R. and D.R., unpublished data). We show here that paracrine expression alone enhances migration compared with simultaneous paracrine and autocrine expression (Fig. 8D). However, if no paracrine expression is present, cells expressing periostin in an autocrine fashion are more likely to migrate than cells that lack periostin. The migratory function is also interesting with respect to expression of periostin in tumour development and metastasis. The ability of tumour cells to migrate and invade other tissues is an important prerequisite for the development of metastasis (Hanahan and Weinberg, 2000). Papers with conflicting results have been published showing that upregulation as well as downregulation of periostin can lead to a more severe tumour phenotype and to enhanced metastasis (Kim et al., 2005; Malanchi et al., 2011; Morra and Moch, 2011). This leads us to propose a model in which the periostin expression levels of the tumour itself, the periostin expression levels of the surrounding tissue and the periostin levels in the serum cooperatively influence the metastatic potential of a tumour.

We showed that the expression levels of periostin are not only influenced by TGFβ-1, as previously shown (Horiuchi et al., 1999), but also by NRG1. Additionally, the interaction of the two ligands results in a higher expression level than either ligand on its own (Fig. 5E). Experiments using different conditions have shown that the neuregulin signalling and TGFβ-1 can cooperate to influence the invasiveness of cancer cells (He et al., 2011), and also in peripheral nerve regeneration (Ribeiro-Resende et al., 2009). Both of these studies suggest the existence of cooperative, synergistic effects for

Journal of Cell Science (2015) 128, 3345-3355 doi:10.1242/jcs.174177

TGFβ-1 and neuregulin signalling. From our results, it is very possible that these effects are mediated through periostin. In recent experiments, it has been shown that Wnt5a can also upregulate periostin expression but seems to exert this upregulation solely through augmentation of TGFβ-1 levels (Hasegawa et al., 2015). The connection between neuregulins and the expression level of periostin, as well as our preliminary data on nerve regeneration, are exciting as a recent paper shows that re-expression of neuregulins after injury to Schwann cells is highly important for regeneration and remyelination (Stassart et al., 2013).

Our results show that periostin exists in a variety of isoforms and that its expression levels are influenced cooperatively by different ligands of receptor kinases. Furthermore, periostin can interact with different ECM molecules, and these interactions are most likely to affect the localisation of periostin. Therefore, this study suggests that periostin is a protein that is involved in cell motility, the exact function of which can be fine-tuned through expression levels, interaction partners and also possibly different isoforms.

MATERIALS AND METHODS

Transgenic mice

Generation, maintenance and genotyping of mice heterozygous for a deletion in *ErbB3* has been described previously (Riethmacher et al., 1997), whereas generation and genotyping of periostin-deficient mice will be described elsewhere (A. Brodarac, Impaired tooth development in periostin deficient mice, PhD thesis, University of Hamburg, 2006). All animals in Hamburg were cared for according to the 'Guide for the Care and Use of Laboratory Animals' prepared by the National Academy of Sciences and published by the National Institutes of Health (NIH; publication 86-23 revised 1985), and experiments involving animals bred in Southampton were performed under a Home Office Licence and in accordance with the Animals (Scientific Procedures) Act, 1986, UK.

DRG cultures

Heterozygous mutant animals were mated, and pregnant females euthanized at 12.5 dpc. The embryonic DRG were dissected and grown in a defined medium that has been used previously for embryonic mouse neurons (Davies, 1998). Genotyping was performed using standard techniques with the following primers – ErbB3 forward-1 5′-GGGTGTCTGAGTC-TTTGAAGCTGGAG-3′, reverse-1 5′-ACCTGTAATCTCCCGACTGT-CCTGAA-3′, reverse-2 5′-CGAATTCGCCAATGACAAGACGCTGG-3′; Periostin forward-1 5′-TGTGGTGGCAGAGACAGAAG-3′, reverse-1 5′-CTCCCCTGTGGTGCATTTAC-3′, reverse-2 5′-GTTGCACCACAG-ATGAAACG-3′.

Cell culture

S16 cells were maintained in Dulbecco's modified Eagle's medium that had been supplemented with heat-inactivated 10% fetal calf serum. All cell culture reagents were purchased from Invitrogen unless otherwise specified. TGFβ-1 from porcine platelets as well as collagen I, collagen IV, collagen V and fibronectin were purchased from Sigma. NRG1 was purchased from Neomarkers, and Laminin-1 from Roche Applied Science. The anti-periostin antibody was an affinity purified polyclonal antibody from rabbit directed against the first 347 amino acids of the protein without the leader sequence. The monoclonal Sox10 antibody was provided by Michael Wegner (University of Erlangen, Germany).

Isoform analysis

DRG explant cultures were cultivated for 36 h, and total RNA was extracted using Trizol (Invitrogen). Reverse transcription was performed with Superscript II (Invitrogen) and oligo(dT) primer. Transcribed cDNA was amplified using periostin-specific primers F15 and R23 (forward primer 5′-CATCCACGTCGTGGACAAACTCCTC-3′, reverse primer 5′-T-TGGCTTCTGTTGGTTGTCA-3′) and purified by using agarose gel electrophoresis. The amplicons were isolated and then subcloned into pGemT easy vectors (Promega); the constructs were subsequently sequenced.

Microarray hybridisation

DRG explant cultures were cultivated for 36 h, and total RNA was isolated using Trizol (Invitrogen), according to the manufacturer's instructions. RNA was reverse transcribed using a T7-promoter-tagged polyT primer [5′-GGCCAGTGAATTGTAATACGACTCACTATAGGGA-GGCGG-$(dT)_{24}$-3′], and antisense RNA was produced using T7 RNA polymerase. Antisense RNA was examined by using gel electrophoresis. Equivalent amounts of RNA from five age-matched embryos of the same genotype were pooled to generate a microarray probe. Probes were biotin-labelled in a second round of T7 amplification, as previously described (Luo et al., 1999). Profiles of ErbB3-deficient mice were compared with the profiles of wild-type littermates of the same genetic background. Microarray profiling was performed in triplicate from independent preparations of embryonic RNA using Affymetrix MG-U74Av2, MG-U74Bv2 and MG-U74Cv2 GeneChips (36,000 sequences). Data were normalized, and comparative analyses were performed using the statistical algorithm of Affymetrix Microarray Suite (MAS) 5.0 software following the manufacturer's guidelines. Ranking and filtering of genes was performed using Microsoft Excel.

Virtual northern blot

Total RNA from DRG cultures was transcribed with oligo-dT primer by reverse transcriptase and amplified using the SMART™ technology (Clontech) following the manufacturer's guidelines. Thereafter, Southern blots were performed using the first 582 nucleotides of the periostin cDNA or full-length GAPDH labelled with [^{32}P]-CTP.

In situ hybridisation and immunohistochemistry

Embryos were isolated at 10–16.5 dpc from staged pregnancies and fixed in 4% paraformaldehyde (PFA; in PBS) for 4–16 h. Samples were then equilibrated in 30% sucrose, embedded in OCT (Miles), frozen and sectioned using a cryostat. *In situ* hybridisation was performed as described previously (Sonnenberg et al., 1991). The first 582 nucleotides of periostin were used as periostin-specific probe.

For immunohistochemistry, embryos and tissues were fixed in 4% PFA in PBS at 4°C overnight, cryoprotected in 20% sucrose in PBS for 12 h at 4°C, embedded in OCT compound (Miles) and sectioned using a cryostat (thickness of 10 µm). Sections were rinsed three times with PBS, blocked for 30 min with PBS containing 0.1% Triton X-100 and 0.2% bovine serum albumin (BSA) and incubated overnight with primary antibodies at 4°C. After being washed three times with PBS (each wash lasting 5 min), the sections were incubated with the appropriate secondary antibodies conjugated to Alexa 466 (Molecular Probes) or Cy3 (Jackson Laboratories; Chemicon) for 1 h and then washed. Primary mouse immunoglobulin G1 antibodies were detected with Zenon technology (Molecular Probes). After the sections had been rinsed with PBS and nuclei had been counterstained with 4′,6′-diamidino-2-phenylindole (DAPI; 0.001 mg/ml of PBS), sections were examined with a Zeiss Axioplan 2 microscope, and images were taken with a Zeiss AxioCam digital camera (Brockschnieder et al., 2004). In the case of double-labelling experiments, slides were fixed in 4% PFA (in PBS) for 30 min after the final wash. Then the second primary antibody was added, and the procedure described above was followed through again. The following antibodies were used in this study: anti-Sox10 (monoclonal antibody from Michael Wegner's Lab); anti-periostin (Abcam); anti-β-galactosidase (Cappel); anti-laminin (Lab Vision Corporation).

Expression of recombinant proteins

Total RNA from DRG cultures was transcribed with oligo-dT primer 5′-GACCACGCGTATCGATGTCGAC-$(dT)_{16}$-3′ by reverse transcriptase. Periostin cDNA was amplified by using gene specific primers 5′-GGCT-GAAGATGGTTCCTCTC-3′ and a primer binding to the overhang of the oligo-dT primer (5′-GACCAGGCGTATCGATGTCGAC-3′). For recombinant protein expression, the cDNA was amplified with primers 5′-GATCGCTAGCATGGTTCCTCTCCTG-3′ and 5′-GATCGCGGCCGC-CTGAGAACGGCCTTC-3′ providing *Nhe*I and *Not*I restriction sites, respectively. The PCR product was purified by using agarose gel electrophoresis and inserted into pcDNA5/FRT (Invitrogen) providing a 10×His and a c-Myc tag at the 3′-end. In order to generate stable lines, Flp-In HEK-293 cells (Invitrogen) were transfected with the expression vector

using jet PEI (Q BIO gene) following the manufacturer's guidelines. This cell line enables the rapid generation of stable expression from a defined locus. The protein was purified from the supernatant by using immobilized metal ion affinity chromatography using Ni-NTA-matrix (Qiagen) following the manufacturer's guidelines and was then dialyzed against PBS.

Quantitative real-time PCR

Total RNA for qRT-PCR analyses was extracted from S16 cells that had been cultured for 24 h on laminin-coated plates in Opti-Mem medium and subsequently stimulated with 10 ng/ml NRG1 or 1 ng/ml TGFβ-1 for 24 h. After treatment with RNase-free DNase for 30 min at 37°C to remove genomic DNA, the quantity and quality of the RNA was determined by using the RNA 6000 Nano LabChip Kit (Agilent). The cDNA was synthesised from 3 µg of total RNA using 1 µg random primers with Superscript II (Invitrogen) and spiked with the *amylose extender1* (ae I) gene from wheat. qRT-PCR was performed using the ABI PRISM 7700 (ABI). The efficiency of cDNA synthesis was evaluated by amplifying the ae I cDNA (ae I forward 5′-ACGCGATGCCCTCCATAG-3′, ae I reverse 5′-AATTCGAGACCGGATCCT-3′). All reactions contained 15 ng cDNA, 300 nM periostin forward primer 5′-TTCCGAGAGATCATCCAACC-3′, 50 nM periostin reverse primer 5′-AGGCTGAGGAAGATGCTGAA-3′ (product size 82 bp), 18S 60 nM forward primer 5′-CGGCTACCACATCC-AAGAA-3′, 18S 60 nM reverse primer 5′-GCTGGAATTACCGCGGCT-3′ (product size 182 bp) and QPCR Mastermix for SYBR® Green I (Eurogentec) in a final volume of 20 µl. Primer concentrations and conditions were optimised in preliminary experiments. The thermal profile started with an initial step of 50°C for 2 min, followed by 10 min 95°C to activate the polymerase and subsequently 40 cycles each comprising 15 s 95°C and 1 min 65°C. In each analysis, all samples were run in parallel. The control gene selected to normalize each sample for RNA content was 18S ribosomal RNA. The fold difference was analysed by using the standard deviation calculations using the relative standard curve method. The paired sample *t*-test was used to evaluate the significance of differences in expression in paired groups.

Western blot analysis and immunoprecipitation

Cells were washed twice with ice-cold PBS and lysed with a buffer containing 50 mM Tris-HCl (pH 7.4), 150 NaCl, 1% Nonidet P-40, 1 mM phenylmethylsulfonyl fluoride and a protease inhibitor cocktail (Complete mini, Roche). Protein extracts or purified protein were separated by using SDS-PAGE, transferred to PVDF membrane (Millipore), blocked with 5% milk powder in PBS and incubated with the indicated antibodies overnight. Immunoreactive bands were visualized by using chemiluminescence (Millipore). For immunoprecipitation, the HEK-293 cells were transfected with a plasmid expressing periostin or β-galactosidase. Laminin was added to the cell culture medium and, at 24 h after transfection, the supernatant was collected and precleared with protein-G/A–Sepharose (Santa Cruz Biotechnology) for 2 h at 4°C. The pre-cleared supernatant was incubated with anti-laminin antibody (1:100) (Clone A5, NeoMarkers) overnight. The immunocomplex was extensively washed, the samples (30 µg) were subjected to immunoblotting, and periostin was detected with anti-c-Myc antibody (clone 9E10, Sigma).

Solid-phase assay

96-well plates (Nunc) were coated overnight with 100 µg/ml of collagen I, collagen IV, collagen V, fibronectin, bovine serum albumin fraction V (Sigma) and laminin (Roche). After blocking with 5% milk powder in 100 mM Tris-HCl pH 7.5, 150 mM NaCl, 200 ng/ml of recombinantly expressed and purified periostin was incubated for 5 h in 100 mM Tris-HCl pH 7.5, 150 mM NaCl or 100 mM Tris-HCl pH 7.5, 150 mM NaCl, 2 mM $CaCl_2$. Periostin was detected using an anti-c-Myc horseradish peroxidase (HRP) conjugate. The immunoreactivity was visualized by using ABTS as a substrate and measured at 405 nm.

Migration analysis

For the migration assay, HEK-293 cells were transfected for 36 h with plasmid encoding periostin or β-galactosidase. The conditioned medium was collected and filtered. Additionally, HEK-293 cells were transfected for 24 h with plasmids encoding periostin or EGFP. 1×10^5 of these cells were then transferred onto 8-µm pore polycarbonate filter (Nunc). The lower chamber of Transwell inserts was loaded with the conditioned medium. After 24 h of incubation, the top cells on the Transwell membrane were removed using Q-tips. The cells trapped by the membrane were fixed and stained with Diff-Quick (Düdingen, Switzerland). Cell numbers within the entire membrane area were determined.

For the analyses of Schwann cell migration, DRG explant cultures were cultured for 72 h and were then analysed by immunofluorescence using an antibody against Sox10 and the Neurofilament 200 antibody (Sigma) to visualise Schwann cells and axons, respectively. All migrating Sox10-positive cells per DRG were counted.

BrdU incorporation in cultured DRG

The DRG explant cultures were cultured for 48 h and incubated for 1 h with 10 µM BrdU, washed with PBS and fixed for 20 min with Carnoy's fixative (methanol and acetic acid, 3:1) at −20°C. Subsequently, the DRG cultures were incubated for 15 min with 2.4 M HCl at 37°C. To identify incorporated BrdU, thus proliferating cells, an antibody against BrdU (Roche) was used.

TUNEL staining

The DRG were cultured for 48 h and fixed with 1% PFA (in PBS) for 10 min at room temperature. To identify apoptotic cells, the ApopTag Apoptosis detection kit (Q-BIOgene) was used following the manufacturer's guidelines.

Statistical analysis

In all experiments, appropriate statistical analysis (ANOVA, *t*-test) was performed using GraphPad Prism 4 or MiniTab (Release 15) software. Data are shown as mean values with standard errors of the mean.

Acknowledgements

We thank Andreja Brodarac (Center for Molecular Neurobiology, University of Hamburg, Hamburg, Germany) for her involvement in the generation of the periostin-deficient mouse strain. We thank Michael Wegner for the Sox10 antibody.

Competing interests

The authors declare no competing or financial interests.

Author contributions

M.M. performed most of the experiments. E.S.-R. helped with experiments involving animal material. D.R. and E.-R.-S. designed the experiments, helped to analyse the data and wrote the manuscript. All authors discussed the data.

Funding

This work was supported by the Bundesministerium für Bildung und Forschung (BMBF) within the framework of the Nationales Genomforschungsnetzwerk (NGFN) [grant number 01GS0119 to D.R.].

References

Bao, S., Ouyang, G., Bai, X., Huang, Z., Ma, C., Liu, M., Shao, R., Anderson, R. M., Rich, J. N. and Wang, X.-F. (2004). Periostin potently promotes metastatic growth of colon cancer by augmenting cell survival via the Akt/PKB pathway. *Cancer Cell* **5**, 329-339.

Bornstein, P. and Sage, E. H. (2002). Matricellular proteins: extracellular modulators of cell function. *Curr. Opin. Cell Biol.* **14**, 608-616.

Britsch, S., Li, L., Kirchhoff, S., Theuring, F., Brinkmann, V., Birchmeier, C. and Riethmacher, D. (1998). The ErbB2 and ErbB3 receptors and their ligand, neuregulin-1, are essential for development of the sympathetic nervous system. *Genes Dev.* **12**, 1825-1836.

Brockschnieder, D., Lappe-Siefke, C., Goebbels, S., Boesl, M. R., Nave, K.-A. and Riethmacher, D. (2004). Cell depletion due to diphtheria toxin fragment A after Cre-mediated recombination. *Mol. Cell. Biol.* **24**, 7636-7642.

Buchstaller, J., Sommer, L., Bodmer, M., Hoffmann, R., Suter, U. and Mantei, N. (2004). Efficient isolation and gene expression profiling of small numbers of neural crest stem cells and developing Schwann cells. *J. Neurosci.* **24**, 2357-2365.

Chernousov, M. A., Stahl, R. C. and Carey, D. J. (2001). Schwann cell type V collagen inhibits axonal outgrowth and promotes Schwann cell migration via distinct adhesive activities of the collagen and noncollagen domains. *J. Neurosci.* **21**, 6125-6135.

Chernousov, M. A., Yu, W.-M., Chen, Z.-L., Carey, D. J. and Strickland, S. (2008). Regulation of Schwann cell function by the extracellular matrix. *Glia* **56**, 1498-1507.
Crane, J. F. and Trainor, P. A. (2006). Neural crest stem and progenitor cells. *Annu. Rev. Cell Dev. Biol.* **22**, 267-286.
Davies, A. M. (1998). Neuronal survival: early dependence on Schwann cells. *Curr. Biol.* **8**, R15-R18.
Dupin, E., Calloni, G., Real, C., Goncalves-Trentin, A. and Le Douarin, N. M. (2007). Neural crest progenitors and stem cells. *C. R. Biol.* **330**, 521-529.
Elkins, T., Hortsch, M., Bieber, A. J., Snow, P. M. and Goodman, C. S. (1990). Drosophila fasciclin I is a novel homophilic adhesion molecule that along with fasciclin III can mediate cell sorting. *J. Cell Biol.* **110**, 1825-1832.
Garratt, A. N., Voiculescu, O., Topilko, P., Charnay, P. and Birchmeier, C. (2000). A dual role of erbB2 in myelination and in expansion of the schwann cell precursor pool. *J. Cell Biol.* **148**, 1035-1046.
Gillan, L., Matei, D., Fishman, D. A., Gerbin, C. S., Karlan, B. Y. and Chang, D. D. (2002). Periostin secreted by epithelial ovarian carcinoma is a ligand for alpha(V) beta(3) and alpha(V)beta(5) integrins and promotes cell motility. *Cancer Res.* **62**, 5358-5364.
Hanahan, D. and Weinberg, R. A. (2000). The hallmarks of cancer. *Cell* **100**, 57-70.
Hasegawa, D., Wada, N., Maeda, H., Yoshida, S., Mitarai, H., Tomokiyo, A., Monnouchi, S., Hamano, S., Yuda, A. and Akamine, A. (2015). Wnt5a induces collagen production by human periodontal ligament cells through TGFbeta1-mediated upregulation of periostin expression. *J. Cell Physiol.* **230**, 2647-2660.
He, Y., Northey, J. J., Primeau, M., Machado, R. D., Trembath, R., Siegel, P. M. and Lamarche-Vane, N. (2011). CdGAP is required for transforming growth factor beta- and Neu/ErbB-2-induced breast cancer cell motility and invasion. *Oncogene* **30**, 1032-1045.
Horiuchi, K., Amizuka, N., Takeshita, S., Takamatsu, H., Katsuura, M., Ozawa, H., Toyama, Y., Bonewald, L. F. and Kudo, A. (1999). Identification and characterization of a novel protein, periostin, with restricted expression to periosteum and periodontal ligament and increased expression by transforming growth factor beta. *J. Bone Miner. Res.* **14**, 1239-1249.
Isono, T., Kim, C. J., Ando, Y., Sakurai, H., Okada, Y. and Inoue, H. (2009). Suppression of cell invasiveness by periostin via TAB1/TAK1. *Int. J. Oncol.* **35**, 425-432.
Jessen, K. R. and Mirsky, R. (2005). The origin and development of glial cells in peripheral nerves. *Nat. Rev. Neurosci.* **6**, 671-682.
Kii, I., Amizuka, N., Minqi, L., Kitajima, S., Saga, Y. and Kudo, A. (2006). Periostin is an extracellular matrix protein required for eruption of incisors in mice. *Biochem. Biophys. Res. Commun.* **342**, 766-772.
Kii, I., Nishiyama, T., Li, M., Matsumoto, K.-I., Saito, M., Amizuka, N. and Kudo, A. (2010). Incorporation of tenascin-C into the extracellular matrix by periostin underlies an extracellular meshwork architecture. *J. Biol. Chem.* **285**, 2028-2039.
Kim, C. J., Yoshioka, N., Tambe, Y., Kushima, R., Okada, Y. and Inoue, H. (2005). Periostin is down-regulated in high grade human bladder cancers and suppresses in vitro cell invasiveness and in vivo metastasis of cancer cells. *Int. J. Cancer* **117**, 51-58.
Kruzynska-Frejtag, A., Machnicki, M., Rogers, R., Markwald, R. R. and Conway, S. J. (2001). Periostin (an osteoblast-specific factor) is expressed within the embryonic mouse heart during valve formation. *Mech. Dev.* **103**, 183-188.
Kyutoku, M., Taniyama, Y., Katsuragi, N., Shimizu, H., Kunugiza, Y., Iekushi, K., Koibuchi, N., Sanada, F., Oshita, Y. and Morishita, R. (2011). Role of periostin in cancer progression and metastasis: inhibition of breast cancer progression and metastasis by anti-periostin antibody in a murine model. *Int. J. Mol. Med.* **28**, 181-186.
Li, J.-S., Sun, G. W., Wei, X. Y. and Tang, W. H. (2007). Expression of periostin and its clinicopathological relevance in gastric cancer. *World J. Gastroenterol.* **13**, 5261-5266.
Lindsley, A., Li, W., Wang, J., Maeda, N., Rogers, R. and Conway, S. J. (2005). Comparison of the four mouse fasciclin-containing genes expression patterns during valvuloseptal morphogenesis. *Gene Expr. Patterns* **5**, 593-600.
Litvin, J., Selim, A.-H., Montgomery, M. O., Lehmann, K., Rico, M. C., Devlin, H., Bednarik, D. P. and Safadi, F. F. (2004). Expression and function of periostin-isoforms in bone. *J. Cell. Biochem.* **92**, 1044-1061.
Luo, L., Salunga, R. C., Guo, H., Bittner, A., Joy, K. C., Galindo, J. E., Xiao, H., Rogers, K. E., Wan, J. S., Jackson, M. R. et al. (1999). Gene expression profiles of laser-captured adjacent neuronal subtypes. *Nat. Med.* **5**, 117-122.
Lv, Y., Wang, W., Jia, W.-D., Sun, Q.-K., Li, J.-S., Ma, J.-L., Liu, W.-B., Zhou, H.-C., Ge, Y.-S., Yu, J.-H. et al. (2013). High-level expression of periostin is closely related to metastatic potential and poor prognosis of hepatocellular carcinoma. *Med. Oncol.* **30**, 385.
Lyons, D. A., Pogoda, H.-M., Voas, M. G., Woods, I. G., Diamond, B., Nix, R., Arana, N., Jacobs, J. and Talbot, W. S. (2005). erbb3 and erbb2 are essential for schwann cell migration and myelination in zebrafish. *Curr. Biol.* **15**, 513-524.
Malanchi, I., Santamaria-Martínez, A., Susanto, E., Peng, H., Lehr, H.-A., Delaloye, J.-F. and Huelsken, J. (2011). Interactions between cancer stem cells and their niche govern metastatic colonization. *Nature* **481**, 85-89.
Michailov, G. V., Sereda, M. W., Brinkmann, B. G., Fischer, T. M., Haug, B., Birchmeier, C., Role, L., Lai, C., Schwab, M. H. and Nave, K.-A. (2004). Axonal neuregulin-1 regulates myelin sheath thickness. *Science* **304**, 700-703.
Milner, R., Wilby, M., Nishimura, S., Boylen, K., Edwards, G., Fawcett, J., Streuli, C., Pytela, R. and ffrench-Constant, C. (1997). Division of labor of Schwann cell integrins during migration on peripheral nerve extracellular matrix ligands. *Dev. Biol.* **185**, 215-228.
Morra, L. and Moch, H. (2011). Periostin expression and epithelial-mesenchymal transition in cancer: a review and an update. *Virchows Arch.* **459**, 465-475.
Newbern, J. and Birchmeier, C. (2010). Nrg1/ErbB signaling networks in Schwann cell development and myelination. *Semin. Cell Dev. Biol.* **21**, 922-928.
Norris, R. A., Damon, B., Mironov, V., Kasyanov, V., Ramamurthi, A., Moreno-Rodriguez, R., Trusk, T., Potts, J. D., Goodwin, R. L., Davis, J. et al. (2007). Periostin regulates collagen fibrillogenesis and the biomechanical properties of connective tissues. *J. Cell. Biochem.* **101**, 695-711.
Norris, R. A., Borg, T. K., Butcher, J. T., Baudino, T. A., Banerjee, I. and Markwald, R. R. (2008). Neonatal and adult cardiovascular pathophysiological remodeling and repair: developmental role of periostin. *Ann. N. Y. Acad. Sci.* **1123**, 30-40.
Oka, T., Xu, J., Kaiser, R. A., Melendez, J., Hambleton, M., Sargent, M. A., Lorts, A., Brunskill, E. W., Dorn, G. W., II, Conway, S. J. et al. (2007). Genetic manipulation of periostin expression reveals a role in cardiac hypertrophy and ventricular remodeling. *Circ. Res.* **101**, 313-321.
Ozdemir, C., Akpulat, U., Sharafi, P., Yildiz, Y., Onbasilar, I. and Kocaefe, C. (2014). Periostin is temporally expressed as an extracellular matrix component in skeletal muscle regeneration and differentiation. *Gene* **553**, 130-139.
Puglisi, F., Puppin, C., Pegolo, E., Andreetta, C., Pascoletti, G., D'Aurizio, F., Pandolfi, M., Fasola, G., Piga, A., Damante, G. et al. (2008). Expression of periostin in human breast cancer. *J. Clin. Pathol.* **61**, 494-498.
Ribeiro-Resende, V. T., Koenig, B., Nichterwitz, S., Oberhoffner, S. and Schlosshauer, B. (2009). Strategies for inducing the formation of bands of Bungner in peripheral nerve regeneration. *Biomaterials* **30**, 5251-5259.
Riethmacher, D., Sonnenberg-Riethmacher, E., Brinkmann, V., Yamaai, T., Lewin, G. R. and Birchmeier, C. (1997). Severe neuropathies in mice with targeted mutations in the ErbB3 receptor. *Nature* **389**, 725-730.
Rios, H., Koushik, S. V., Wang, H., Wang, J., Zhou, H.-M., Lindsley, A., Rogers, R., Chen, Z., Maeda, M., Kruzynska-Frejtag, A. et al. (2005). periostin null mice exhibit dwarfism, incisor enamel defects, and an early-onset periodontal disease-like phenotype. *Mol. Cell. Biol.* **25**, 11131-11144.
Sasaki, H., Auclair, D., Fukai, I., Kiriyama, M., Yamakawa, Y., Fujii, Y. and Chen, L. B. (2001a). Serum level of the periostin, a homologue of an insect cell adhesion molecule, as a prognostic marker in nonsmall cell lung carcinomas. *Cancer* **92**, 843-848.
Sasaki, H., Lo, K.-M., Chen, L. B., Auclair, D., Nakashima, Y., Moriyama, S., Fukai, I., Tam, C., Loda, M. and Fujii, Y. (2001b). Expression of Periostin, homologous with an insect cell adhesion molecule, as a prognostic marker in non-small cell lung cancers. *Jpn. J. Cancer Res.* **92**, 869-873.
Sasaki, H., Yu, C.-Y., Dai, M., Tam, C., Loda, M., Auclair, D., Chen, L. B. and Elias, A. (2003). Elevated serum periostin levels in patients with bone metastases from breast but not lung cancer. *Breast Cancer Res. Treat.* **77**, 245-252.
Shao, R., Bao, S., Bai, X., Blanchette, C., Anderson, R. M., Dang, T., Gishizky, M. L., Marks, J. R. and Wang, X.-F. (2004). Acquired expression of periostin by human breast cancers promotes tumor angiogenesis through up-regulation of vascular endothelial growth factor receptor 2 expression. *Mol. Cell. Biol.* **24**, 3992-4003.
Shimazaki, M. and Kudo, A. (2008). Impaired capsule formation of tumors in periostin-null mice. *Biochem. Biophys. Res. Commun.* **367**, 736-742.
Snider, P., Hinton, R. B., Moreno-Rodriguez, R. A., Wang, J., Rogers, R., Lindsley, A., Li, F., Ingram, D. A., Menick, D., Field, L. et al. (2008). Periostin is required for maturation and extracellular matrix stabilization of noncardiomyocyte lineages of the heart. *Circ. Res.* **102**, 752-760.
Sonnenberg, E., Godecke, A., Walter, B., Bladt, F. and Birchmeier, C. (1991). Transient and locally restricted expression of the ros1 protooncogene during mouse development. *EMBO J.* **10**, 3693-3702.
Stassart, R. M., Fledrich, R., Velanac, V., Brinkmann, B. G., Schwab, M. H., Meijer, D., Sereda, M. W. and Nave, K.-A. (2013). A role for Schwann cell-derived neuregulin-1 in remyelination. *Nat. Neurosci.* **16**, 48-54.
Tai, I. T., Dai, M. and Chen, L. B. (2005). Periostin induction in tumor cell line explants and inhibition of in vitro cell growth by anti-periostin antibodies. *Carcinogenesis* **26**, 908-915.
Takayama, G., Arima, K., Kanaji, T., Toda, S., Tanaka, H., Shoji, S., McKenzie, A. N. J., Nagai, H., Hotokebuchi, T. and Izuhara, K. (2006). Periostin: a novel component of subepithelial fibrosis of bronchial asthma downstream of IL-4 and IL-13 signals. *J. Allergy Clin. Immunol.* **118**, 98-104.

Journal of Cell Science

Takeshita, S., Kikuno, R., Tezuka, K. and Amann, E. (1993). Osteoblast-specific factor 2: cloning of a putative bone adhesion protein with homology with the insect protein fasciclin I. *Biochem. J.* **294**, 271-278.

Taveggia, C., Zanazzi, G., Petrylak, A., Yano, H., Rosenbluth, J., Einheber, S., Xu, X., Esper, R. M., Loeb, J. A., Shrager, P. et al. (2005). Neuregulin-1 type III determines the ensheathment fate of axons. *Neuron* **47**, 681-694.

Toda, K., Small, J. A., Goda, S. and Quarles, R. H. (1994). Biochemical and cellular properties of three immortalized Schwann cell lines expressing different levels of the myelin-associated glycoprotein. *J. Neurochem.* **63**, 1646-1657.

Yan, W. and Shao, R. (2006). Transduction of a mesenchyme-specific gene periostin into 293T cells induces cell invasive activity through epithelial-mesenchymal transformation. *J. Biol. Chem.* **281**, 19700-19708.

Yoshioka, N., Fuji, S., Shimakage, M., Kodama, K., Hakura, A., Yutsudo, M., Inoue, H. and Nojima, H. (2002). Suppression of anchorage-independent growth of human cancer cell lines by the TRIF52/periostin/OSF-2 gene. *Exp. Cell Res.* **279**, 91-99.

Zinn, K., McAllister, L. and Goodman, C. S. (1988). Sequence analysis and neuronal expression of fasciclin I in grasshopper and Drosophila. *Cell* **53**, 577-587.